

COMPUTATIONALLY EFFICIENT ROBUST WIDELY LINEAR BEAMFORMING FOR IMPROPER NON-STATIONARY SIGNALS

Ted Kronvall, Naveed R. Butt, and Andreas Jakobsson

Centre for Mathematical Sciences, Lund University, Box 118, SE-22100 Lund, Sweden.
email: {ted, naveed, aj}@maths.lth.se

ABSTRACT

In this work, we introduce a computationally efficient Kalman-filter based implementation of the robust widely linear (WL) minimum variance distortionless response (MVDR) beamformer. The beamformer is able to achieve the same performance as the recently derived robust WL MVDR beamformer, but avoids the computationally burdensome solution based on a second order cone programming (SOCP), and exploiting the recent Kalman-based regular robust MVDR beamformer, extends this to also allow for non-circular sources and interferences. Numerical simulations illustrate the achieved performance.

Index Terms— Widely linear estimation, robust Capon beamforming, constrained Kalman filter, time-variant filtering, non-circular signals

1. INTRODUCTION

Adaptive beamforming plays an important role in a large variety of applications, including, for example, wireless communications, radar, sonar, astronomy, seismology, medical imaging and microphone array speech processing [1–5]. Most of the commonly used optimal beamformers belong to a class of linear time-invariant filters that are developed under the implicit assumption that the measured signal is second order (SO) circular [6]. This includes the well-known Capon’s minimum variance distortionless response (MVDR) beamformer and its many robust variants (see, e.g., [7] and the references therein), all of which are known to perform well when the measured signal is indeed SO circular [8]. Unfortunately, the SO circularity assumption does not hold true for many signals of practical importance. For instance, many signals in radio communication systems, such as amplitude modulation (AM), binary phase-shift keying (BPSK), and minimum shift keying (MSK) are in fact non-circular, and the application of standard linear beamformers to these signals leads to suboptimal performance [9]. To better deal with non-circular signals, several optimal widely linear (WL) MVDR beamformers have been developed in the last decade, exploiting

the information contained in the complementary covariance matrix, describing the dependence between the signal and its complex conjugate (see, e.g., [9, 10]). While these optimal WL MVDR algorithms outperform their linear counterparts when the measured signal is non-circular, they, similarly to linear MVDR methods, exhibit extreme sensitivity to mismatch between the assumed and the actual array responses to the signal-of-interest (SOI). In practical applications, such mismatches typically take place due to look direction errors, array calibration errors, mutual coupling, or limited sample support. In a more recent work, robust WL beamformers that allows for the typical pointing errors in the assumed steering vector of the SOI have been developed and shown to lead to improved performance [11]. However, an important limitation of the developed robust WL beamformers is their high computational complexity, often making online implementation infeasible. To alleviate this problem, we here introduce a computationally efficient robust WL MVDR by generalizing the Kalman-filter based standard robust beamformer of [12] to also allow for non-circularity of both the SOI and the interferers. This is achieved by exploiting the complementary covariance matrix of the measured signal and by introducing additional constraints based on the non-circularity of the SOI. Using realistic BPSK signals, the proposed approach, hereafter referred to as the Kalman-based WL robust Capon beamformer (KWL-RCB), is shown to achieve similar performance as the robust WL beamformers of [11], hereafter WL-RCB, albeit at a much reduced computational cost. A further advantage of the proposed approach, is its ability to handle both stationary and non-stationary interference sources.

2. ROBUST WL MVDR BEAMFORMER

Consider an array of L sensors, receiving a narrow-band signal, $s(t)$, corrupted by noise and other interferences, such that the $L \times 1$ snapshot vector for the array can be detailed as

$$\mathbf{x}(t) = s(t)\mathbf{a} + \mathbf{n}(t) \quad (1)$$

where t denotes the time index, $t = 1, \dots, M$, $s(t)$ the complex envelope of the SOI, $\mathbf{a} \in \mathcal{C}^{L \times 1}$ the complex steering vector of the SOI, and $\mathbf{n}(t)$ represents the interference-plus-noise

This work was supported in part by the Swedish Research Council and Carl Trygger’s foundation.

component. Allowing both the SOI and the interferences to be SO non-circular, and assuming that the interferences are zero-mean and uncorrelated with the SOI, the full SO statistics of the $\mathbf{x}(t)$ may be given in terms of its covariance matrix, $\mathbf{R}_x \in \mathcal{C}^{L \times L}$, and its complementary covariance matrix, $\mathbf{C}_x \in \mathcal{C}^{L \times L}$, as

$$\begin{aligned} \mathbf{R}_x &\triangleq \mathbb{E} \{ \mathbf{x}_t \mathbf{x}_t^H \} = \pi_s \mathbf{a} \mathbf{a}^H + \mathbf{R}_n \triangleq \mathbf{R}_s + \mathbf{R}_n \quad (2) \\ \mathbf{C}_x &\triangleq \mathbb{E} \{ \mathbf{x}_t \mathbf{x}_t^T \} = \pi_s \gamma_s \mathbf{a} \mathbf{a}^T + \mathbf{C}_n \triangleq \mathbf{C}_s + \mathbf{C}_n \quad (3) \end{aligned}$$

where $(\cdot)^T$ and $(\cdot)^H$ denote the transpose and the Hermitian transpose, respectively. Here $\mathbf{R}_n = \mathbb{E} \{ \mathbf{n}(t) \mathbf{n}(t)^H \}$ and $\mathbf{C}_n = \mathbb{E} \{ \mathbf{n}(t) \mathbf{n}(t)^T \}$ represents the covariance and the complementary covariance matrices of \mathbf{n}_t , respectively, whereas $\pi_s = \mathbb{E} \{ |s(t)|^2 \}$ and $\gamma_s = \mathbb{E} \{ s(t)^2 \} / \pi_s$ denotes the power of the signal $s(t)$ and the non-circularity coefficient of the SOI, respectively. The non-circularity coefficient, γ_s , gives a measure of the non-circularity of the SOI, with $\gamma_s = 0$ representing a SO circular source, whereas $\gamma_s = 1$ indicates that the SOI is on a line in the complex plane. Furthermore, by virtue of its definition, $|\gamma_s| \leq 1$. It is worth noting that, in the case when \mathbf{x} is SO stationary, $\gamma_s = 0$ and $\mathbf{C}_n = 0$, and consequently, the complementary covariance matrix \mathbf{C}_x vanishes, leading to the standard linear case. Given $\mathbf{x}(t)$, the commonly used linear MVDR (Capon) beamformer gives the output

$$y(t) = \mathbf{w}^H \mathbf{x}(t) \quad (4)$$

where the linear time-invariant filter, $\mathbf{w} \in \mathcal{C}^{L \times 1}$, is formed by minimizing the output power of the filter, while constraining the filter to have unit gain in the look direction, i.e.,

$$\hat{\mathbf{w}}_{\text{opt}} = \arg \min_{\mathbf{w}} \mathbf{w}^H \mathbf{R}_x \mathbf{w} \quad \text{s.t.} \quad \mathbf{w}^H \mathbf{a} = 1 \quad (5)$$

$$= \mathbf{R}_x^{-1} \mathbf{a} (\mathbf{a}^H \mathbf{R}_x^{-1} \mathbf{a})^{-1} \quad (6)$$

where \mathbf{R}_x is typically replaced by the outer-product sample covariance matrix estimate. As is clear from (5), the standard MVDR formulation does not take the complementary covariance matrix \mathbf{C}_x into account, and therefore, not surprisingly, suffers from severe performance degradation when the signal is non-circular. To remove this deficiency, and to exploit the possible non-circularity of the measured signal, a WL MVDR technique was introduced in [10], reformulating the minimization to instead operate on the augmented snapshot vector, $\tilde{\mathbf{x}}(t)$, defined as

$$\tilde{\mathbf{x}}(t) = \begin{bmatrix} \mathbf{x}(t)^T & \mathbf{x}(t)^H \end{bmatrix}^T \quad (7)$$

$$= s(t) \tilde{\mathbf{a}}_1 + s^*(t) \tilde{\mathbf{a}}_2 + \tilde{\mathbf{n}}(t) \quad (8)$$

where $\tilde{\mathbf{a}}_1 = \begin{bmatrix} \mathbf{a}^T & \mathbf{0}_N^T \end{bmatrix}^T$, $\tilde{\mathbf{a}}_2 = \begin{bmatrix} \mathbf{0}_N^T & \mathbf{a}^T \end{bmatrix}^T$, and with $(\cdot)^*$ denoting the complex conjugate. The SO statistics for the augmented snapshot may then be given as

$$\begin{aligned} \mathbf{R}_{\tilde{\mathbf{x}}} &= \begin{bmatrix} \mathbf{R}_x & \mathbf{C}_x \\ \mathbf{C}_x^* & \mathbf{R}_x^* \end{bmatrix} = \begin{bmatrix} \mathbf{R}_s & \mathbf{C}_s \\ \mathbf{C}_s^* & \mathbf{R}_s^* \end{bmatrix} + \begin{bmatrix} \mathbf{R}_n & \mathbf{C}_n \\ \mathbf{C}_n^* & \mathbf{R}_n^* \end{bmatrix} \\ &\triangleq \mathbf{R}_{\tilde{\mathbf{s}}} + \mathbf{R}_{\tilde{\mathbf{n}}} \quad (9) \end{aligned}$$

Assuming that the augmented snapshot vector $\tilde{\mathbf{x}}$ is passed through a filter, $\tilde{\mathbf{w}} \in \mathcal{C}^{2L \times 1}$, one may, using the above definitions, write the filter output as

$$y(t) = \tilde{\mathbf{w}}^H \tilde{\mathbf{x}}(t) = s(t) \tilde{\mathbf{w}}^H \tilde{\mathbf{a}}_1 + s(t)^* \tilde{\mathbf{w}}^H \tilde{\mathbf{a}}_2 + \tilde{n}^F(t) \quad (10)$$

where $\tilde{n}^F(t)$ represents the filtered noise sequence. Using (9) and (10), the WL MVDR beamformer may be formulated as

$$\min_{\tilde{\mathbf{w}}} \tilde{\mathbf{w}}^H \mathbf{R}_{\tilde{\mathbf{x}}} \tilde{\mathbf{w}} \quad \text{s.t.} \quad \tilde{\mathbf{w}}^H \tilde{\mathbf{A}} = \begin{bmatrix} 1 & 0 \end{bmatrix} \quad (11)$$

where $\tilde{\mathbf{A}} = \begin{bmatrix} \tilde{\mathbf{a}}_1 & \tilde{\mathbf{a}}_2 \end{bmatrix}$, which has the solution [9]

$$\hat{\tilde{\mathbf{w}}}_{\text{opt}} = \mathbf{R}_{\tilde{\mathbf{x}}}^{-1} \tilde{\mathbf{A}} \left(\tilde{\mathbf{A}}^H \mathbf{R}_{\tilde{\mathbf{x}}}^{-1} \tilde{\mathbf{A}} \right)^{-1} \begin{bmatrix} 1 \\ 0 \end{bmatrix} \quad (12)$$

The resulting WL MVDR beamformer has been shown to provide better signal-to-noise-and-interference ratio (SINR) as compared to its linear counterpart, given in (6), when the measured signal is non-circular [9]. In many applications, the non-circularity of the SOI may be approximately known, allowing the beamformer to be extended to incorporate such knowledge. To do so, one may, following [13], decompose γ_s and $s(t)^*$ as

$$s^*(t) = \gamma_s^* s(t) + \pi_s (1 - |\gamma_s|)^{1/2} s'(t) \quad (13)$$

where the signal $s'(t)$ is orthogonal to $s(t)$. Inserting (13) into (8) yields the augmented snapshot vector

$$\begin{aligned} \tilde{\mathbf{x}}(t) &= s(t) (\tilde{\mathbf{a}}_1 + \gamma_s^* \tilde{\mathbf{a}}_2) + \\ &\quad + s'(t) \left(\pi_s (1 - |\gamma_s|)^{1/2} \right) \tilde{\mathbf{a}}_2 + \tilde{\mathbf{n}}(t) \quad (14) \end{aligned}$$

$$\triangleq s(t) \tilde{\mathbf{a}}_\gamma + \tilde{\mathbf{n}}_\gamma(t) \quad (15)$$

and the WL beamformer output

$$y(t) = \tilde{\mathbf{w}}^H \tilde{\mathbf{x}}(t) = s(t) \tilde{\mathbf{w}}^H \tilde{\mathbf{a}}_\gamma + \tilde{\mathbf{n}}_\gamma^F(t) \quad (16)$$

Using (16), the optimal WL MVDR beamformer can thus be reformulated as [13]

$$\min_{\tilde{\mathbf{w}}} \tilde{\mathbf{w}}^H \mathbf{R}_{\tilde{\mathbf{x}}} \tilde{\mathbf{w}}, \quad \text{s.t.} \quad \tilde{\mathbf{w}}^H \tilde{\mathbf{a}}_\gamma = 1 \quad (17)$$

taking non-circularity of the SOI into account.

3. PROPOSED KALMAN IMPLEMENTATION

Reminiscent to the standard MVDR beamformer, the resulting optimal WL MVDR beamformer will be sensitive to errors in the assumed steering vector of the SOI. In [11], the WL-RCB was shown to provide improved signal to interference plus noise ratio (SINR) performance in case of errors in the SOI steering vector. Unfortunately, similar to the conventional beamformers, the robust WL beamformers requires solving a second order cone programming (SOCP) problem,

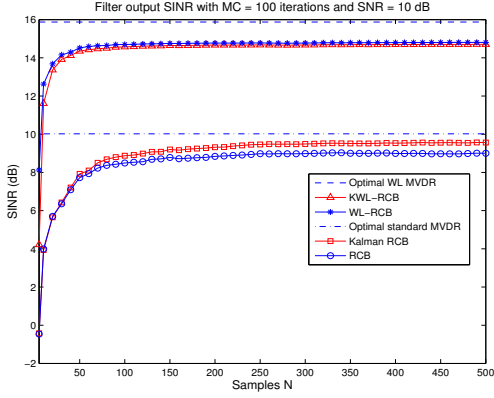


Fig. 1. Output SINR as a function of sample length for non-circular BPSK signals with SNR = 10 dB. Red triangles and blue asterisks are robust WL beamformers and perform equally, while the former, the proposed Kalman implementation, has reduced complexity.

having a complexity of about $\mathcal{O}(L^3)$, restricting their applicability for online or otherwise time-restricted applications. To alleviate this problem, we here develop KWL-RCB, reminiscent of the Kalman-based standard RCB developed in [12], and thereby also yielding an implementation of complexity $\mathcal{O}(L^2)$. To achieve this, it can be noted that the robustness constraint on $\tilde{\mathbf{a}}_\gamma$, as given in (17), can be formulated in terms of the errors in the assumed SOI steering vector, $\tilde{\mathbf{a}}$, and the assumed SOI non-circularity coefficient, $\tilde{\gamma}_s$. To do so, let the true SOI steering vector, \mathbf{a} , lie within a small hypersphere of radius ϵ_a , centered around the assumed steering vector, $\tilde{\mathbf{a}}$, as

$$\|\mathbf{a} - \tilde{\mathbf{a}}\|^2 \leq \epsilon_a \quad (18)$$

and, similarly, allow γ_s to lie on a small interval of radius ϵ_γ , centered around the assumed value $\tilde{\gamma}_s$, as

$$|\gamma_s - \tilde{\gamma}_s|^2 \leq \epsilon_\gamma \quad (19)$$

Using (18) and (19), a necessary constraint on $\tilde{\mathbf{a}}_\gamma$ may be formulated as [11]

$$\epsilon_1 = \|\tilde{\mathbf{a}}_\gamma - \tilde{\mathbf{a}}_{\tilde{\gamma}_s}\|^2 \quad (20)$$

$$= \left\| \begin{bmatrix} \mathbf{a} - \tilde{\mathbf{a}} \\ \gamma_s^* \mathbf{a}^* - \tilde{\gamma}_s^* \tilde{\mathbf{a}}^* \end{bmatrix} \right\|^2 \quad (21)$$

$$\leq \|\mathbf{a} - \tilde{\mathbf{a}}\|^2 + \|\gamma_s^* \mathbf{a}^* - \tilde{\gamma}_s^* \tilde{\mathbf{a}}^*\|^2 \quad (22)$$

$$\leq \epsilon_a + \left(\tilde{\gamma}_s \sqrt{\epsilon_{\text{epsilon}_a}} + \sqrt{N} \sqrt{\epsilon_\gamma} + \sqrt{\epsilon_a} \sqrt{\epsilon_\gamma} \right)^2 \quad (23)$$

Imposing the constraint in (20) on the minimization in (17), and carrying out algebraic manipulations similar to those in [14], leads to the worst-case robust WL MVDR formulation

$$\min_{\tilde{\mathbf{w}}} \tilde{\mathbf{w}}^H \mathbf{R}_x \tilde{\mathbf{w}} \quad \text{s.t.} \quad \tilde{\mathbf{w}}^H \tilde{\mathbf{a}}_\gamma \geq \sqrt{\epsilon_1} \|\tilde{\mathbf{w}}\| + 1 \quad (24)$$

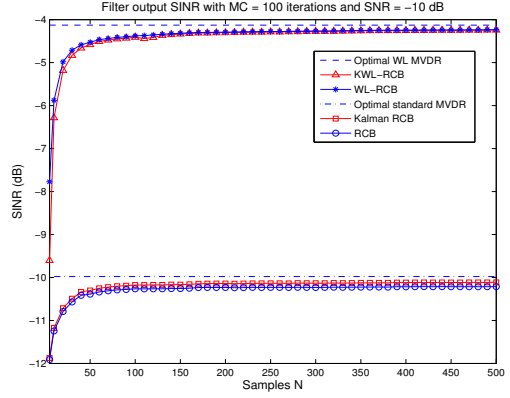


Fig. 2. Output SINR as a function of sample length for non-circular BPSK signals with SNR = -10 dB. Red triangles and blue asterisks are robust WL beamformers and perform equally, while the former, the proposed Kalman implementation, has reduced complexity.

which may be rewritten as an equivalent minimum mean square error (MMSE) estimation problem for the augmented weight vector

$$\min_{\tilde{\mathbf{w}}} \text{E} [|0 - \tilde{\mathbf{x}}(k)^H \tilde{\mathbf{w}}(k)|^2] \quad \text{s.t.} \quad h_2(\tilde{\mathbf{w}}(k)) = 1 \quad (25)$$

where the cost function penalizes the deviation of the beamformer output from an ideal (zero) signal, and

$$h_2(\tilde{\mathbf{w}}(k)) = \epsilon_1 \tilde{\mathbf{w}}^H \tilde{\mathbf{w}} - |\tilde{\mathbf{w}}^H \tilde{\mathbf{a}}_\gamma|^2 + \tilde{\mathbf{w}}^H \tilde{\mathbf{a}}_\gamma + \tilde{\mathbf{a}}_\gamma^H \tilde{\mathbf{w}} \quad (26)$$

Reminiscent to the derivation in [12], one may thus use this reformulation to derive an efficient Kalman-filter based implementation of (25), by letting the weight vector of the robust WL MVDR, $\tilde{\mathbf{w}}(k)$, evolve as a first-order Markov process

$$\tilde{\mathbf{w}}(k+1) = \lambda \tilde{\mathbf{w}}(k) + \mathbf{e}(k) \quad (27)$$

where $\mathbf{e}(k)$ denotes a zero-mean white Gaussian innovation process, with covariance matrix $\mathbf{Q} = \text{E} \{ \mathbf{e}(k) \mathbf{e}(k)^H \} = \sigma_s^2 \mathbf{I}_{2M}$, with λ denoting a user parameter. The observed states then details the filter output and the mismatch of the assumed $\tilde{\mathbf{a}}_\gamma$, such that

$$\mathbf{z} \triangleq \begin{bmatrix} 0 \\ 1 \end{bmatrix} = \begin{bmatrix} \tilde{\mathbf{w}}(k)^H \tilde{\mathbf{x}}(k) + v_1(k) \\ h_2(\tilde{\mathbf{w}}(k)) + v_2(k) \end{bmatrix} \quad (28)$$

$$\triangleq \mathbf{h}(\tilde{\mathbf{w}}(k)) + \mathbf{v}(k)$$

where $v_1(k)$ and $v_2(k)$ are assumed to be independent zero-mean white Gaussian noise processes with SO statistics

$$\mathbf{R}_v = \text{E} \{ \mathbf{v}(k) \mathbf{v}(k)^H \} = \begin{bmatrix} \sigma_1^2 & 0 \\ 0 & \sigma_2^2 \end{bmatrix} \quad (29)$$

Since the observation equation in (28) is non-linear in the estimation vector $\tilde{\mathbf{w}}(k)$, the SO extended Kalman filter of [15]

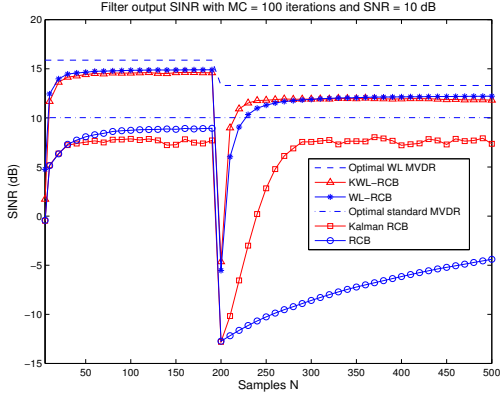


Fig. 3. Output SINR as a function of sample length for non-stationary BPSK signals at SNR = 10 dB. At $N = 200$ the arrival direction of the interference change and the beamformers tries to adjust correspondingly. The figure shows how Kalman based beamformers deals with non-stationarity faster than SOCP based beamformers.

may be used to find the recursive update equation for the adaptive $\tilde{\mathbf{w}}(k)$ estimates as

$$\hat{\tilde{\mathbf{w}}}(k) = \lambda \hat{\tilde{\mathbf{w}}}(k-1) + \mathbf{G}_k (z - \hat{z}(k|k-1)) \quad (30)$$

where $\mathbf{G}(k)$ is the Kalman filter gain

$$\mathbf{G}(k) = \mathbf{P}(k|k-1) \nabla_{\tilde{\mathbf{w}}} \mathbf{h}(\hat{\tilde{\mathbf{w}}}(k-1)) \mathbf{S}(k)^{-1} \quad (31)$$

and where $\hat{z}(k|k-1)$ denote the one-step prediction of the observation, given by (32), given at the top of next page, where $\mathbf{P}(\cdot)$ and $\mathbf{S}(k)$ are the weight vector and the innovation covariance matrices, respectively, being formed as (33), given at the top of next page, and

$$\mathbf{P}(k|k-1) = \lambda^2 \mathbf{P}(k-1|k-1) + \mathbf{Q} \quad (34)$$

where $\nabla_{\tilde{\mathbf{w}}} \mathbf{h}(\tilde{\mathbf{w}}(k))$ and $\nabla_{\tilde{\mathbf{w}}}^2 \mathbf{h}(\tilde{\mathbf{w}}(k))$ are the first and second order derivatives of \mathbf{h} with respect to $\tilde{\mathbf{w}}$, given by

$$\begin{aligned} \nabla_{\tilde{\mathbf{w}}} \mathbf{h}(\tilde{\mathbf{w}}(k)) &= \begin{bmatrix} \tilde{\mathbf{x}}(k)^H \\ \epsilon_1 \tilde{\mathbf{w}}(k)^H - (\tilde{\mathbf{a}}_\gamma \tilde{\mathbf{a}}_\gamma^H \tilde{\mathbf{w}}(k))^H + \tilde{\mathbf{a}}_\gamma^H \end{bmatrix} \\ \nabla_{\tilde{\mathbf{w}}}^2 \mathbf{h}(\tilde{\mathbf{w}}(k)) &= \begin{bmatrix} \mathbf{0}_{2M} \\ \epsilon_1 \mathbf{I}_{2M} - \tilde{\mathbf{a}}_\gamma \tilde{\mathbf{a}}_\gamma^H \end{bmatrix} \triangleq \begin{bmatrix} \nabla_{\tilde{\mathbf{w}}}^2 \mathbf{h}^{(1)} \\ \nabla_{\tilde{\mathbf{w}}}^2 \mathbf{h}^{(2)} \end{bmatrix} \end{aligned}$$

Finally, the covariance matrix of the weight vector may be updated as

$$\mathbf{P}(k) = \mathbf{P}(k|k-1) - \mathbf{G}(k) \mathbf{S}(k) \mathbf{G}(k)^H \quad (35)$$

The user parameters λ and σ_s^2 should be chosen to reflect the operating environment, e.g., for non-stationary signals one may choose $\lambda \geq 1$ and $\sigma_s^2 > 0$, to allow for the optimal weight vectors to change over time.

4. NUMERICAL RESULTS

In this section, we examine the performance of the proposed KWL-RCB, examining the output SINR, which for WL filters, taking the non-circularity into account, is given as [13]

$$\text{SINR}(\tilde{\mathbf{w}}) = \frac{\pi_s |\tilde{\mathbf{w}}^H \tilde{\mathbf{a}}_\gamma|^2}{\tilde{\mathbf{w}}^H \mathbf{R}_{\tilde{\mathbf{n}}_\gamma} \tilde{\mathbf{w}}} \quad (36)$$

and analogously for the linear beamformers. Similarly, the optimal output SINR is defined as

$$\text{SINR}(\tilde{\mathbf{w}}_{\text{opt}}) = \pi_s \tilde{\mathbf{a}}_\gamma^H \mathbf{R}_{\tilde{\mathbf{n}}_\gamma}^{-1} \tilde{\mathbf{a}}_\gamma \quad (37)$$

and, again, analogously for the linear beamformers. Initially, we consider a uniform linear array (ULA), with $L = 2$ sensors, on which two BPSK signals impinge, originating from direction 0° and 30° , respectively, being corrupted by a temporally and spatially white noise. The signal-to-noise ratio (SNR), defined as $\sigma^2 \sigma_n^{-2}$, where σ^2 and σ_n^2 denote the signal and noise power, respectively, of the two signals are 10 dB respective 20 dB. The first source is deemed to be the SOI, and has a non-circularity coefficient of $\gamma_s = -0.5 + i0.866$, whereas the second source, deemed to be an interference source, has a non-circularity coefficient of $\gamma_n = 1$. A total of $N = 500$ measurements at SNR = 10 dB are used to form the estimate, which is more than enough to reach convergence. To evaluate the robustness of the beamformer, the assumed steering vector is set to 3° and the mismatch in non-circularity is randomly set to 0.001, consequently giving ϵ_1 as in (20). Figure 1 shows the output SINR of four different beamformers, namely the KWL-RCB, as compared with the WL-RCB [11], and, as a comparison, the linear Kalman RCB [12] and the regular RCB [16]. The beamformers are compared to the theoretically optimal SINRs, being $\{15.87, 10.02\}$ dB, which is an upper limit if there would be no mismatch in \mathbf{a} and γ_s . As seen from the figure, both KWL-RCB and the WL-RCB perform equally well, and similarly to what is shown in [12], this also holds for the linear beamformers. Performance is thus shown to be maintained although the Kalman-based beamformers have reduced complexity, allowing for an efficient time-updating of the estimates as additional samples becomes available.

For the same simulation setting, only changing the signal power to be SNR = -10 dB, figure 2 shows the SINR of the four beamformers introduced, yielding consequent results. The theoretically optimal SINRs are in this setting $\{-4.21, -7.59\}$ dB, and for both simulations, we have set $\sigma_1^2 = \|\tilde{\mathbf{w}}\|^2 (2L\sigma^2 + \sigma_n^2)$, $\sigma_2^2 = 0.2$, $\lambda = 1$, and, as the DOA of the BPSK signals are not expected to change over time, $\sigma_s^2 = 0$.

Extending the signal environment to allow for non-stationarity, the same signals as above are simulated up to $N = 200$, when the arrival direction of the interfering BPSK signal instantaneously changes from 30° to -30° . To allow

$$\hat{\mathbf{z}}(k|k-1) = \begin{bmatrix} \lambda \tilde{\mathbf{x}}(k)^H \hat{\mathbf{w}}(k-1) \\ h_2(\lambda \hat{\mathbf{w}}(k-1)) - \frac{1}{2} \text{tr}(\nabla_{\hat{\mathbf{w}}}^2 \mathbf{h}^{(2)} \mathbf{P}(k|k-1)) \end{bmatrix} \quad (32)$$

$$\mathbf{S}(k|k-1) = \nabla_{\hat{\mathbf{w}}} \mathbf{h}(\lambda \hat{\mathbf{w}}(k-1)) \mathbf{P}(k|k-1) \cdot \nabla_{\hat{\mathbf{w}}} \mathbf{h}(\lambda \hat{\mathbf{w}}(k-1))^H + \frac{1}{2} \begin{bmatrix} 0 & 0 \\ 0 & 1 \end{bmatrix} \text{tr}(\nabla_{\hat{\mathbf{w}}}^2 \mathbf{h}^{(2)} \mathbf{P}(k|k-1) \cdot \nabla_{\hat{\mathbf{w}}}^2 \mathbf{h}^{(2)} \mathbf{P}(k|k-1)) + \mathbf{R}_v \quad (33)$$

for the possibility of such changes, σ_s is set to 10^{-6} , trading of stability for ability to change over time. Figure 2 shows how KWL-RCB is able to adjust faster to non-stationary changes than the SOCP-based WL-RCB. Throughout the simulations, we have, as was done in [11], set the error bounds as $\check{\epsilon}_1 = 1.2 \cdot \epsilon_1$, and $\check{\epsilon}_a = 1.2 \cdot \epsilon_a$. Although, as was shown in [11, 16], the performance of the discussed beamformers is relatively insensitive to this choice.

5. ACKNOWLEDGEMENT

We wish to express our gratitude towards the authors of [11] and [12], for kindly contributing with code for their implementations.

6. REFERENCES

- [1] H. Cox, R. M. Zeskind, and M. M. Owen, "Robust Adaptive Beamforming," *IEEE Trans. Acoust., Speech, Signal Process.*, vol. 35, no. 10, pp. 1365–1376, Oct. 1987.
- [2] M. Elmer, B.D. Jeffs, Karl F. Warnick, J.R. Fisher, and R.D. Norrod, "Beamformer design methods for radio astronomical phased array feeds," *Antennas and Propagation, IEEE Transactions on*, vol. 60, no. 2, pp. 903–914, Feb. 2012.
- [3] Weiziu Du and R.L. Kirlin, "Exploration seismic applications of high resolution beamforming methodology," in *Statistical Signal and Array Processing, 1992. Conference Proceedings., IEEE Sixth SP Workshop on*, 1992, pp. 428–431.
- [4] J.-F. Synnevåg, A. Austeng, and S. Holm, "Adaptive Beamforming Applied to Medical Ultrasound Imaging," *IEEE Trans. Ultrason., Ferroelectr., Freq. Control*, vol. 54, no. 8, pp. 1606–1613, august 2007.
- [5] D. B. Ward and G. W. Elko, "Mixed nearfield/farfield beamforming: A new technique for speech acquisition in a reverberant environment," in *IEEE Acoustics, Speech, and Signal Processing Workshop on Applications of Signal Processing to Audio and Acoustics*, New Paltz, NY, October 1997, p. 4.
- [6] B. Picinbono, "On circularity," *IEEE Trans. Signal Process.*, vol. 42, no. 12, pp. 3473–3482, Dec. 1994.
- [7] P. Stoica and J. Li, *Robust adaptive beamforming*, John Wiley & Sons, 2005.
- [8] P. Stoica and R. Moses, *Spectral Analysis of Signals*, Prentice Hall, Upper Saddle River, N.J., 2005.
- [9] P. Chevalier and A. Blin, "Widely Linear MVDR Beamformers for the Reception of an Unknown Signal Corrupted by Noncircular Interferences," *IEEE Trans. Signal Process.*, vol. 55, no. 11, pp. 5323–5336, Nov. 2007.
- [10] T. McWhorter and P. Schreier, "Widely-linear beamforming," in *Conference Record of the Thirty-Seventh Asilomar Conference on Signals, Systems and Computers*, 9–12 Nov. 2003, vol. 1, pp. 753–759.
- [11] Guohua Wang, Joni Polili Lie, and Chong-Meng Samson See, "A Robust Approach to Optimum Widely Linear MVDR Beamformers," in *Acoustics, Speech and Signal Processing (ICASSP), 2012 IEEE International Conference on*, March, pp. 2593–2596.
- [12] A. El-Keyi, T. Kirubarajan, and A.B. Gershman, "Robust adaptive beamforming based on the kalman filter," *Signal Processing, IEEE Transactions on*, vol. 53, no. 8, pp. 3032–3041, Aug.
- [13] P. Chevalier, J.-P. Delmas, and A. Oukaci, "Optimal widely linear MVDR beamforming for noncircular signals," in *Proc. IEEE International Conference on Acoustics, Speech and Signal Processing ICASSP 2009*, 19–24 April 2009, pp. 3573–3576.
- [14] S. A. Vorobyov, A. B. Gershman, and Z.-Q. Luo, "Robust Adaptive Beamforming Using Worst-Case Performance Optimization: A Solution to the Signal Mismatch Problem," *IEEE Trans. Signal Process.*, vol. 51, no. 2, pp. 313–324, February 2003.
- [15] Y. Bar-Shalom and X.-R. Li, *Estimation and Tracking: Principles, Techniques, and Software*, Artech House, 1993.
- [16] P. Stoica, Z. Wang, and J. Li, "Robust Capon Beamforming," *IEEE Signal Process. Lett.*, vol. 10, no. 6, pp. 172–175, June 2003.